Copyright © 2009 Tech Science Press CMES, vol.48, no.1, pp.27-41, 2009

Shell Buckling of Carbon Nanotubes Using Nanoindentation

L. Munteanu[1] **and V. Chiroiu**[1]

Abstract: The long-range nanoindentation response of carbon nanotubes is studied using a new method that combines the features of Nonlocal Theory and Molecular Mechanics. The deformation of compressed multiple walled carbon nanotubes is investigated, with the emphasis on the simulation of the nanoindentation technique in order to compare the present method to available experimental results.

Keywords: Carbon nanotubes; Molecular mechanics; Nonlocal theory; Buckling; Nanoindentation.

1 Introduction

Indentation is a testing method which is routinely used for the evaluation of the mechanical properties of materials [Oliver and Pharr 1992, Johnson 1985; Dumitriu and Chiroiu 2006; Dumitriu, Gauchs and Chiroiu 2008]. The deformation mechanism is size dependent. For example, the spreading of intershell distances and the inlayer van der Waals interactions in CNTs depend on the tube size [Nair, Farkas and Kriz 2008; Kiang, Endo, Ajayan, G. Dresselhaus and M.S.Dresselhaus 1998]. With different dimensions and geometries of CNTs, the mechanical properties of CNTs are also size dependent [Chen, Cheng and Hsu 2007, Chiroiu, Munteanu and Donescu 2006]. The surface energy significantly affects the stress concentration around the holes as the size of the holes shrinks to nanometers, meanwhile the interaction between the holes also influences the stress distribution around the holes, which become evident as the holes close to each other [Hu and Shen 2008].

There are many works reported in the modeling of CNTs which have extensively been reviewed by Guz, Rushchitsky and Guz (2008), Qian, Wagner, Liu, Yu and Ruoff (2002) and Srivastava and Atluri (2002), Liu (2008). Recently, efficient BEM methods for estimating of the mechanical properties of CNT-based composite are proposed by Araújo and Gray (2008) and Wang and Yao (2008).

[1] Institute of Solid Mechanics of Romanian Academy , Ctin Mille 15, Bucharest 010141

A method which combines Molecular Mechanics with the Finite Element Analysis was introduced by Theodosiou and Saravanos (2007). In this method, repetitive atomic cells were treated as finite elements, whose internal energy is determined by the semi-empirical Brenner molecular potential model. Ling and Atluri (2007) have shown that single wall carbon nanotubes (SWNTs) obey a hyperelastic constitutive model at moderate strains and temperatures, and proposed the Ogden's hyperelasticity model to describe their mechanical behaviors. Transmission between linear and rotational motions and the telescoping behaviors of double-walled carbon nanotubes by atomic-scale finite element and tight-bind Green function methods were discussed by Jiang, Lu and Yu (2008).

Very few experimental results exist on the shell buckling of CNTs, despite its fundamental importance in nanotube mechanics and application. We note in this context the paper of Waters, Gudury, Jouzi and Xu (2005), which analyses the shell buckling of multi-walled carbon nanotubes (MWCNTs) by nanoindentation. Also, a significant discrepancy between the predictions of existing classical theories and the experimental observations highlights the lack of a complete understanding of the role played by the inner walls in MWCNTs mechanics.

Starting with the papers of Waters, Gudury, Jouzi and Xu (2005) and Theodosiou and Saravanos (2007), in this paper a new approach, which combines elements of Nonlocal Theory and Molecular Mechanics, is proposed. The aforementioned method takes advantage of using a continuum theory instead of the finite element method.

The nonlocal theory is grounded for describing long-range interactions among the atoms in CNTs. In such a theory the stress at an atom location is determined by the interatomic interactions in the neighbours around that location [Eringen 1974, Yang, Wong and Qu 2008]. The domain of applicability of a continuum theory depends on the ratio$(\lambda/l,\ \tau/\tau_0)$ or $(\lambda/l, \omega_0/\omega)$, where λ is a characteristic length of the body (atomic distance), l is the external characteristic length associated with the external forces (waves, distances over which load distribution change sharply, geometrical and surface discontinuities), τ the time scale (or frequency ω) which is the minimum transmission time of a signal (or a frequency), and τ_0 is the external characteristic time or frequency) associated with the external forces. All classical theories assume $\lambda/l << 1$ and $\tau/\tau_0 << 1$, i.e. the external forces act simultaneously on a large number of regions, so that these regions interact and the result is a statistical average of the individual responses. For $\lambda/l = 1$ and $\tau/\tau_0 = 1$, the individual fields of intermolecular and atomic forces are important [Eringen 1977].

2 Description of the method

The balance equations in the case of nonlocal continuum mechanics are the same as those corresponding to classical continuum mechanics. Hence the balance equations for a body of volume V enclosed by a surface ∂V, state that the rate of change of the field ϕ (mass, momentum, moment of momentum, energy) in the body, excluding the points on the discontinuity surface σ, which moves into the body with a velocity $\tilde{\mathbf{v}}$ in the direction of its unit normal $\mathbf{n}$, is balanced by the surface flux $\boldsymbol{\tau}$ and the body source g, namely [Eringen 2002]

$$\frac{\mathrm{d}}{\mathrm{d}t}\int\limits_{V-\sigma}\phi\,\mathrm{d}v-\int\limits_{\partial V-\sigma}\boldsymbol{\tau}\cdot\mathrm{d}\mathbf{a}-\int\limits_{\partial V-\sigma}g\,\mathrm{d}v=0, \tag{2.1}$$

By using the Green-Gauss theorem, (1.1) becomes

$$\int\limits_{V-\sigma}[\phi_{,t}+\mathrm{div}(\phi\tilde{\mathbf{v}}-\boldsymbol{\tau})-g]\,\mathrm{d}v+\int\limits_{\sigma}[\phi(\tilde{\mathbf{v}}-\mathbf{v})-\boldsymbol{\tau}]\cdot\mathbf{n}\mathrm{d}a=0, \tag{2.2}$$

where $\phi_{,t}\equiv\partial\phi/\partial t$, $\tilde{\mathbf{v}}$ is the velocity vector, and a bracket denotes the jump of the mentioned quantity at σ. In the classical theory, (1.2) is valid for every part of the body, regardless how small this may be, and the localization condition yields the vanishing of the integrands in the integrals. In the nonlocal theory this assumption is abandoned, however localization is still possible by using certain localization residuals, which must integrate to zero. These residuals are the effects of all other points of the body on one point of the body, i.e. these residuals represent the long-range effects of all points $\mathbf{x}$ at which the balance laws are localized. Therefore, the master balance equations in the case of the nonlocal theory recast as

$$\phi_{,t}+\mathrm{div}(\phi\tilde{\mathbf{v}}-\boldsymbol{\tau})-g=\hat{g}\text{ in }V-\sigma,$$

$$[\phi(\tilde{\mathbf{v}}-\mathbf{v})-\boldsymbol{\tau}]\cdot\mathbf{n}=\hat{G}\text{ on }\sigma, \tag{2.3}$$

subject to

$$\int\limits_{V-\sigma}\hat{g}\mathrm{d}v+\int\limits_{\sigma}\hat{G}\mathrm{da}=0, \tag{2.4}$$

From (1.3) and (1.4), the nonlocal balance equations for the mass, momentum, moment of momentum and energy are given by

$$\rho_{,t}+\mathrm{div}(\rho\tilde{\mathbf{v}})=\hat{\rho},$$

$$\operatorname{div}\mathbf{t}_k + \rho(\mathbf{f} - \dot{\tilde{\mathbf{v}}}) = \hat{\rho}\tilde{\mathbf{v}} - \rho\hat{\mathbf{f}},$$

$$\mathbf{i}_k \times \mathbf{t}_k - \rho(\mathbf{x} \times \hat{\mathbf{f}} - \hat{\mathbf{l}}) = 0,$$

$$-\rho\dot{\varepsilon} + \mathbf{t}_k \cdot \tilde{\mathbf{v}}_{,k} + \nabla \cdot \mathbf{q} + \rho h - \hat{\rho}\left(\varepsilon - \frac{1}{2}\tilde{v} \cdot \tilde{v}\right) - \rho\hat{\mathbf{f}} \cdot \tilde{\mathbf{v}} + \rho\hat{h} = 0,$$

$$\int_V \hat{\rho}\,\mathrm{d}v = 0, \quad \int_V \rho\hat{\mathbf{f}}\,\mathrm{d}v = 0, \quad \int_V \rho\hat{\mathbf{l}}\,\mathrm{d}v = 0, \quad \int_V \rho\hat{h}\,\mathrm{d}v = 0,$$

$$\int_V \hat{\rho}\,\mathrm{d}v = 0, \quad \int_V \rho\hat{\mathbf{f}}\,\mathrm{d}v = 0, \quad \int_V \rho\hat{\mathbf{l}}\,\mathrm{d}v = 0, \quad \int_V \rho\hat{h}\,\mathrm{d}v = 0,$$

where a dot denotes the material time derivative. Here, ρ is the mass density, $\mathbf{t}_k = \mathbf{t}_{kl}\imath_l$ is the stress tensor, $\mathbf{i}_k$ are the Cartesian unit vectors, ε is the internal energy density, $\mathbf{q}$ is the heat flow vector, h is the heat source per unit mass, $\hat{\rho}$ is the mass residual, $\hat{\mathbf{f}}$ is the body force residual, $\hat{\mathbf{l}}$ is the body couple residual, $\hat{h}$ is the energy residual, with the mention that all of the residuals are the nonlocal production of these quantities per unit mass due to the rest of the body.

The second law of thermodynamics is obtained from (1.3), namely

$$\rho\dot{\eta} - \nabla \cdot \mathbf{q} - \frac{\rho h}{\theta} - \rho\hat{b} + \hat{\rho}\eta \geq 0 \text{ in } V - \sigma, \tag{2.5}$$

where η is the entropy density, θ is the absolute temperature and $\hat{b}$ is entropy residual subject to $\int_V \rho\hat{b}\,\mathrm{d}v = 0$.

The following theorems define the elastic nonlocal solid [Eringen 1972]:

THEOREM 2.1. *In the linear theory of nonlocal elastic materials, whose natural state is free of nonlocal effects, the nonlocal body force vanishes, i.e.* $\hat{f}_k = 0$.

THEOREM 2.2. *The constitutive equations for nonlocal linear homogeneous isotropic elastic solids and residuals do not violate the global entropy inequality* (1.5) *if and only if they are of the form*

$$t_{kl} = \lambda e_{rr}\delta_{kl} + 2\mu e_{kl} + \int_{V-\sigma} (\lambda_1' e_{rr}'\delta_{kl} + 2\mu_1' e_{kl}')\mathrm{d}v', \tag{2.6}$$

$$\Sigma = \Sigma_0 + \frac{1}{2}\lambda(e_{kk})^2 + \mu e_{kl} d_{kl} + \int\limits_{V-\sigma} \left(\frac{1}{2}\lambda' e_{kk} e'_{ll} + \mu'_1 e_{kl} e'_{kl}\right) \mathrm{d}v', \tag{2.7}$$

where λ and μ are the classical Lamé elastic constants, and λ' and μ' are the nonlocal Lamé elastic functions which depend on $|\mathbf{x}' - \mathbf{x}|$. Here Σ is the potential functional over all argument functions of $\mathbf{x}'$ covering the entire body, defined by $\rho_0 \psi = \Sigma(\mathbf{x}', \mathbf{x}'_{,k})$, with $\psi = \varepsilon - \theta\eta$ the free energy functional, Σ_0 refers to the value in the natural state, and $\rho_0$the density in the natural state, δ_{kl} is the Kronecher delta, e_{kl} is the strain tensor of the linear theory $2e_{kl} = u_{k,l} + u_{l,k}$and $u_k$are the components of the displacement vector.

A prime placed on quantities indicates that they depend on $\mathbf{x}'$ and $t' \leq t$, where $\mathbf{x}'$ is any other point in the body and t' any time at or prior to present time t. The conditions $\hat{\rho} = 0$ and $\hat{f}_k = 0$ mean that there are no mass and body force nonlocal production in the body.

Other forms of (1.6) and (1.7) are obtained by incorporating λ and μ into λ' and μ'

$$t_{kl} = \int\limits_{V-\sigma} \left[\lambda'(|\mathbf{x}' - \mathbf{x}|) e'_{rr}(\mathbf{x}')\delta_{kl} + 2\mu'(|\mathbf{x}' - \mathbf{x}|) e'_{kl}(\mathbf{x}')\right] \mathrm{d}v'(\mathbf{x}'), \tag{2.8}$$

$$\Sigma = \Sigma_0 + \int\limits_{V-\sigma} \left[\frac{1}{2}\lambda'(|\mathbf{x}' - \mathbf{x}|) e_{kk}(\mathbf{x}) e'_{ll}(\mathbf{x}') + \mu'(|\mathbf{x}' - \mathbf{x}|) e_{kl}(\mathbf{x}) e'_{kl}(\mathbf{x}')\right] \mathrm{d}v'(\mathbf{x}'). \tag{2.9}$$

The *nonlocal Lamé elastic functions* $\lambda'(|\mathbf{x}' - \mathbf{x}|)$ and $\mu'(|\mathbf{x}' - \mathbf{x}|)$ are influence functions, which are positive decreasing functions of $|\mathbf{x}' - \mathbf{x}|$,

$$\lambda'(|\mathbf{x}' - \mathbf{x}|) = \alpha(|\mathbf{x}' - \mathbf{x}|)\lambda,$$

$$\mu(|\mathbf{x}' - \mathbf{x}|) = \alpha(|\mathbf{x}' - \mathbf{x}|)\mu, \tag{2.10}$$

where $\alpha(|\mathbf{x}' - \mathbf{x}|)$ is the nonlocal kernel function which measures the effect of the strain at $\mathbf{x}'$ on the stress at $\mathbf{x}$.

In order to derive the expressions of $\alpha(|\mathbf{x}' - \mathbf{x}|)$ in the case of carbon nanotubes, the potential functional Σ given by (1.9) is identified with the Brenner-Tersoff potential [Brenner 1990, Brenner, Shenderova, Areshkin, Schall and Frankland 2002]. The potential functional Σ is expressed in terms of the repulsive potential $V_R(|\mathbf{x}' - \mathbf{x}|)$, the attractive potential $V_A(|\mathbf{x}' - \mathbf{x}|)$ and the Lennard-Jones potential $V_{dvw}(|\mathbf{x}' - \mathbf{x}|)$

$$\Sigma = \Sigma_0 + \gamma \int\limits_{V-\sigma} [V_R - \beta V_A + V_{vdw}] \mathrm{d}v'(\mathbf{x}'), \tag{2.11}$$

with γ and β the coupling factors, and

$$V_R(|\mathbf{x}'-\mathbf{x}|) = \frac{D_e f_c(|\mathbf{x}'-\mathbf{x}|)}{S-1}\exp\left(-A_1(|\mathbf{x}'-\mathbf{x}|)\right),$$

$$V_A(|\mathbf{x}'-\mathbf{x}|) = \frac{SD_e f_c(|\mathbf{x}'-\mathbf{x}|)}{S-1}\exp\left(-A_2|\mathbf{x}'-\mathbf{x}|)\right),$$

$$V_{vdw} = 4\tilde{\varepsilon}\left[\left(\frac{r_0}{(|\mathbf{x}'-\mathbf{x}|)}\right)^{12} - \left(\frac{r_0}{(|\mathbf{x}'-\mathbf{x}|)}\right)^{6}\right],$$

$$2f_c = (1+\cos\left(\frac{\pi(|\mathbf{x}'-\mathbf{x}|-R_1)}{R_2-R_1}\right),$$

$$f_c(|\mathbf{x}'-\mathbf{x}|) = \begin{cases} 1, & |\mathbf{x}'-\mathbf{x}| < R_1, \\ f_{0c}, & R_1 < |\mathbf{x}'-\mathbf{x}| < R_2, \\ 0, & |\mathbf{x}'-\mathbf{x}| > R_2, \end{cases}$$

where $D_e = 6.32$eV, $S = 1.29$, $\tilde{\varepsilon}$ **is** the energy at the minimum in V_{vdw}, and r_0 is the distance between two atoms at which $V_{vdw} = 0$. For carbon atoms, ε_0 =0.0556 kcal/mol, $r_0 = 3.4$ Å. The function$f_c(|\mathbf{x}'-\mathbf{x}|)$ is an optional "cut-off" function and it may be used to smoothly limit the interactions in (1.11) within a predefined range of neighboring atoms, effectively defined by radii $R_1 = 1.70$? and $R_2 = 2.00$? [Theodosiou and Saravanos 2007]. From (1.9) and (1.11) we obtain an Artan form [Artan 1997]

$$\alpha(|\mathbf{x}'-\mathbf{x}|) = \begin{cases} \sum_{p=1}^{m}\left(B\left(1-\frac{|\mathbf{x}'-\mathbf{x}|}{d}\right)\right)^p, & |\mathbf{x}'-\mathbf{x}| < d, \\ 0, & |\mathbf{x}'-\mathbf{x}| > d. \end{cases} \tag{2.12}$$

where $d = \frac{\delta\sqrt{3}}{\pi}\sqrt{n^2+nm+m^2}$ is the nanotube diameter, $B = 1/d$ and δ is the distance between two neighboring carbon atoms. In an equilibrium state, $\delta \approx 1.42$. The carbon nanotube is described by a geometrical parameter r, $r = na+mb$, where a and b are the lattice unit vectors, and (n,m) is a pair of integers. For $m = 0$ we have a *zigzag form*, for $n = m$we obtain an *armchair form*, while in the general case a *chiral form* is obtained.

3 Nanoindentation simulation

The aim of this study is to simulate the nanoindentation test used by Waters, Gudury, Jouzi and Xu (2005) (with reference to a commercial nanoindenter (TriboIndenter, Hysitron, Minneapolis) with an extremely fine force and displacement resolution ($\sim$300nm and $\sim$1 nm, respectively). A Berkovich three-sided pyramidal tip was used in the present investigation, with a nominal tip radius of 100 nm.

Fig. 1 schematically shows the axially compressed multiple walled carbon nanotube (MWCN) of diameter d =50nm, and length L =100nm, by a nanoindentation technique. The nanotubes used in this study has 15 walls, the outer radius is R_{outer} =25 nm, and the inner radius is R_{inner} =20 nm. The projected contact area for a conical indenter is given by $A = \pi h^2 \tan^2 \theta$, where h is the maximum indentation depth, and θ is the half angle of the indenter. For a Berkovich indenter$A = 24.56h^2$, while for a Vickers indenter $A = 24.50h^2$. For both Berkovich and Vickers indenters $\theta = 70.3^\circ$ [Chollacoop 2004]. Let us denote by $V$the volume of the structure and by S the surface between the indenter and the sample.

The total volume of MWCNT can be defined as the product of the cross-sectional area A_{mw} and the length L [Li and Chou 2003]

$$A_{mw} = \pi[(R_{outer} + 0.17)^2 - (R_{inner} - 0.17)^2], \tag{3.1}$$

where 0.17 is the half layered thickness of the nanotube. The physical response of any point in Vdepends on the state of the entire volume. This dependence can be described by the constitutive laws (1.8) which can be written in the form

$$t_{kl}^{=} \int_V \alpha(|\mathbf{x}' - \mathbf{x}|)\sigma_{kl}^{(}\mathbf{x}')\mathrm{d}v'(\mathbf{x}'), \tag{3.2}$$

where $\sigma_{kl}^{(}\mathbf{x}')$ is the local stress field [Dumitriu and Chiroiu 2006; Civelek, Erdogan and Cakiroglu 1978]

$$\sigma(x) = -\frac{1}{\pi h} \int_{-a}^{a} \int_{-L}^{L} \sigma(t)\varphi(u) \cos\left((t-x)\frac{u}{h}\right) \mathrm{d}u\mathrm{d}t, \tag{3.3}$$

$$\varphi(u) = \frac{\exp(u)[(1+u)\exp(2u) + u - 1]}{\exp(4u) + 4u\exp(2u) - 1}, \quad \int_{-a}^{a} \sigma(t)\mathrm{d}t = P.$$

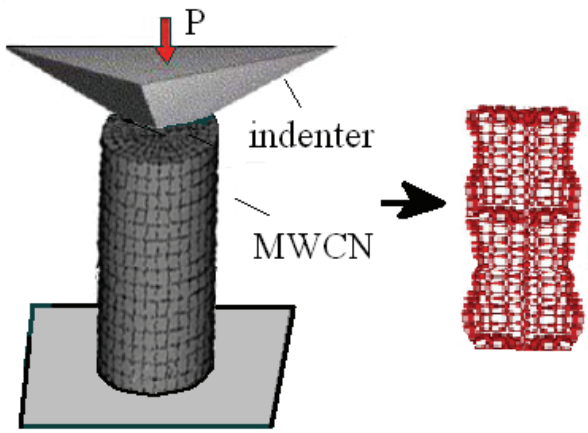

Figure 1: Scheme of the indentation and shell buckling

The nonlocal stress field under the punch is calculated by using (2.2) and (1.12) for $m = 1$,

$$t(x) = \int_{x-d}^{x+d} \left(1 - \frac{|x-x'|}{d}\right) \sigma(x) \mathrm{d}x', \tag{3.4}$$

where $\sigma(x)$ is given by (2.3).

By using the dimensionless quantities $s = t/a$, $q = x/L$, $f(s) = \sigma(as)/\sigma_0$, where$a$ is the contact radius measured at the maximum indentation depth h, eqs. (2.3) and (2.4) become

$$\sigma(x) = -\frac{aL\sigma_0}{\pi h} \int_{-1}^{1}\int_{-1}^{1} f(s)\varphi(qL)\cos\left((as-x)\frac{qL}{h}\right) \mathrm{d}q\mathrm{d}s, \tag{3.5}$$

$$\frac{a}{h}\int_{-1}^{1} f(s)\mathrm{d}s = \frac{P}{h\sigma_0}.$$

Figs. 2 and 3 show the difference between the local (2.5) and nonlocal (2.4) stresses near the boundary of the contact domain for $a/h = 0.5$ and $a/h = 0.3$, respectively. Both figures show that if the points are situated in the neighbourhood of the boundary then the difference between the local and nonlocal solutions cannot be ignored.

The nonlocal stresses are finite at all points of the boundary of the contact domain. The nonlocal stress has a maximum value which is not attained at the boundary of the contact domain.

In order to compare the present results with the experimental results of Waters, Gudury, Jouzi and Xu (2005), we calculate the load-unloaded-displacement curve, as shown in Fig. 4.

As the experiments report, the loading portion consists of three stages: an initial linear increase, then a sudden drop in the slope with the curve becoming flat, and a third stage comprising and increasing load. The sudden decrease in the slope is the signature CNT buckling, which indicates the collapse process illustrated in Fig. 1.

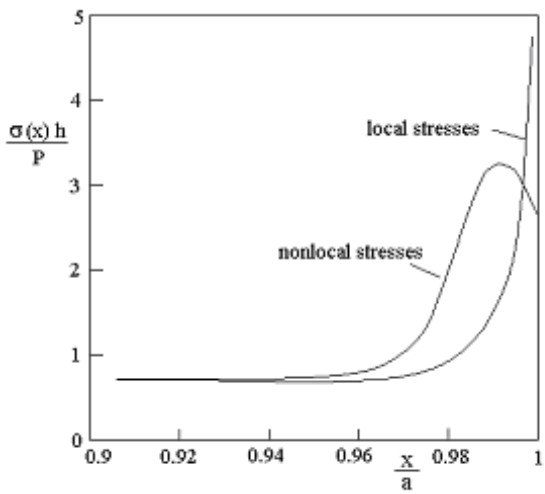

Figure 2: The local and nonlocal stresses near the boundary of the contact domain for $a/h = 0.5$

After buckling, the neighbouring nanotubes come into contact with the indenter tip, which results in an increase in the load, as can be seen from Fig. 4 in the third stage. The position of the zero displacement corresponds to a nonzero load. According to the present theory, the critical buckling is obtained as 2.18μN, which is very close to the experimental result (i.e. in the range 2.0-2.5μN).

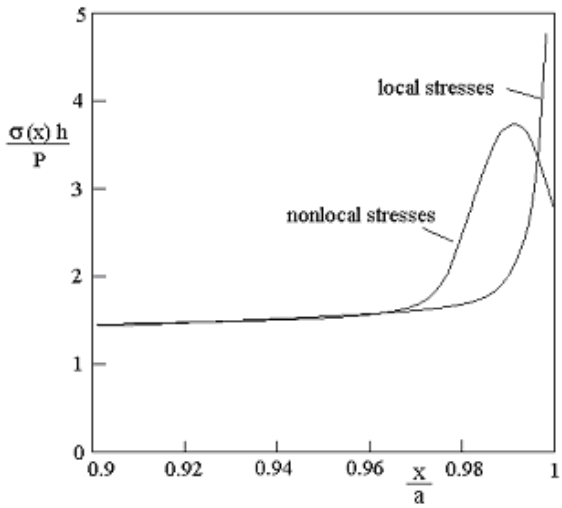

Figure 3: The local and nonlocal stresses near the boundary of the contact domain for $a/h = 0.3$

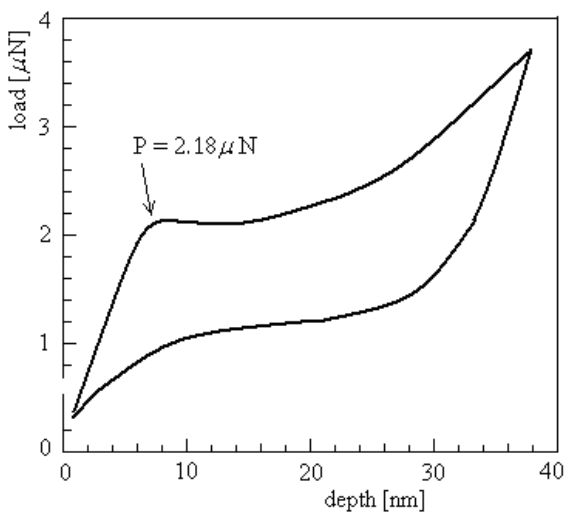

Figure 4: Scheme of the load-unloaded-displacement Curve

4 Evaluation of the Lamé constants

The contact problem for a flat punch is reduced to the integration of the following equation [Solomon 1964]

$$\delta = \tilde{\theta} \iint_D \frac{p(\xi,\eta)}{\sqrt{(x-\xi)^2+(y-\eta)^2}} \mathrm{d}\xi \mathrm{d}\eta \text{ in } D \tag{4.1}$$

with the equilibrium condition

$$P = \iint_D p(\xi,\eta)\mathrm{d}\xi\,\mathrm{d}\eta, \tag{4.2}$$

and the continuity relation

$$p(\xi,\eta) = 0 \text{ on } \partial D, \tag{4.3}$$

where $\tilde{\theta} = \frac{1-\nu}{2\pi\mu}$ is a characteristic constant of the indented material, D is the contact domain, ∂D is the boundary of D, $p(\xi,\eta)$ is the pressure on D (the normal stress exerted by the punch on D), δ is the penetration of the punch into the half-space, P is the applied force, μ is the Coulomb elastic constant and ν is the Poisson's ratio. For given$P$, μ and ν, the problem reduces to finding $p(\xi,\eta)$, δ and D.

One way to solve the problem is to express the pressure $p(\xi,\eta)$from (3.1) as a function of δ and other geometrical parameters that characterise the unknown contact domain$D$, and to determine these parameters, δ and D from (3.2) and (1.3). Finally, the pressure$p(\xi,\eta)$ is determined.

Let us consider that the contact area between the elastic solid and the punch is an unknown convex domain$D$, described by the super-ellipse (or Lamé curve)

$$\left(\frac{x}{a}\right)^n + \left(\frac{y}{b}\right)^n = 1, \quad n > 0, \tag{4.4}$$

where a and b are the radii of the oval shape. The case $n = 2/3$ corresponds to a squashed astroid, $n = 1$ to a squashed diamond, $n = 2$ to an ellipse and $n \to \infty$ to **a** rectangle. The advantage of the super-ellipse consists of the effect of n to rounding the sharp corners. A representation of the super-ellipse in polar coordinates$x = r\cos\theta$,$y = r\sin\theta$, is given by

$$r(\theta) = \left[\left|\frac{\cos\theta}{a}\right|^n + \left|\frac{\sin\theta}{b}\right|^n\right]^{-1/n}, \; 0 \le \theta < \frac{\pi}{2}, \tag{4.5}$$

where

$$r = \frac{\tilde{r}}{\max(a,b)}, \quad 0 \le r \le 1, \quad \tilde{r} = \left[\frac{1}{n}(a^n + b^n)\right]^{1/n}, \quad \lim_{n\to\infty} \tilde{r} = \max(a,b).$$

The following theorems are used for evaluating the Lamé constants for CNTs [Dumitriu and Chiroiu 2006].

THEOREM 4.1. *The solution $p(r)$ of* (3.1) *is a continuous and bounded function at any interior point of the super-elliptical contact domain D*

$$p(r(\theta)) = \left[\frac{3PH^2\mu}{(1-\nu)}\right]^{1/3} \times \left(\frac{1}{2E(\varphi, r\bar{k})}\right)^{2/3} \left(1 - r^2\bar{k}^2\right)^{1/6}. \tag{4.6}$$

The maximum value of the pressure is given by

$$p_{\max} = p(0) = \left[\frac{3PH^2\mu}{(1-\nu)}\right]^{1/3} \times \left(\frac{1}{2E(\pi/2,\bar{k})}\right)^{2/3} \left(1-\bar{k}^2\right)^{1/6}. \tag{4.7}$$

In addition, the pressure vanishes on ∂D.

THEOREM 4.2. *The penetration δ under the punch is given by*

$$\delta = \left[\left(\frac{3}{2}\right)^2 \frac{(1-\nu)^2}{4\pi^2\mu^2} P^2 H\right]^{1/3} \frac{\left(1-\bar{k}^2\right)^{1/3} K(\bar{k})}{E^{1/3}(\bar{k})}. \tag{4.8}$$

In (3.6)-(3.8), H is the main curvature, ν is the Poisson ratio,λ and μ the local Lamé constants, $k = \sqrt{1-\frac{b^2}{a^2}}$ is the eccentricity,

$$\bar{k} = \frac{(n\tilde{r}^n - 2b^n)^{1/n}}{a_m}, \quad a_m = \max(a,b),$$

the integrals $K(k) = \int\limits_0^{\pi\backslash 2} \frac{\mathrm{d}\psi}{\sqrt{1-k^2\sin^2\psi}}$ and $E(k) = \int\limits_0^{\pi/2} \sqrt{1-k^2\sin^2\psi}\mathrm{d}\psi$ are the complete elliptic integrals of the first and second kinds, respectively.

From (3.6)-(3.8), appropriate values for the local Lamé constants for the nanotube can be estimated. For the MWCNT considered in this paper the values μ =2.304 TPa and λ =1.377 TPa (or equivalently the Young modulus Y =5.47 TPa and ν =0.187) are obtained. Based on the continuum assumption, Y can be derived through an axial tension method. The axial elastic modulus Y of the MWCNT can be calculated from the second derivatives of the energy functional with respect to various strains $Y = -\frac{1}{V}\Sigma_{,\varepsilon\varepsilon}$[Chen, Cheng and Hsu 2007] where the cross-sectional area of MWCNTs is defined by (2.1). According to this formula, we obtain Y =5.5TPa. The Poisson ratio can also be estimated by minimizing the energy functional with respect to both the radial compression and the axial extension, and we obtain ν =0.19.

5 Conclusions

In this paper, a new approach which combines elements of Nonlocal Theory and Molecular Mechanics was proposed. The effect of the inlayer van der Waals atomistic interactions for MWCNT was included by means of the Brenner-Tersoff potential. The neighbouring walls of a multi-walled nanotube were coupled through van der Waals interactions, and the "shell" buckling would initiate in the outermost shell, when nanotubes are considered to be short$L/d \sim 1-20$.

The method was applied to simulate the nanoindentation technique for the axially compressed MWCN in order to evaluate the load-unloaded-displacement, the curve critical buckling and the appropriate values for the local Lamé constants. The theoretical results obtained in this paper have been found to be in very good agreement with the experimental data reported by Waters, Gudury, Jouzi and Xu (2005).

The present method can be further extended to investigate the stress-strain relations and the fracture behaviors of S/MWCNT, but these are deferred to future work.

Acknowledgement: The authors are grateful to the National Authority for Scientific Research (ANCS, UEFISCSU), Romania, through PN-II research project nr. 106/2007, code ID_247/2007.

References

Araújo, F.C.; Gray, L.J. (2008): Evaluation of Effective Material Parameters of CNT-reinforced Composites via 3D BEM. *CMES: Computer Modeling in Engineering & Science* **24** (2): 103-121.

Artan, R. (1997): Unsymetrical Elastic Stamp on a Nonlocal Elastic Half Plane, *Computers and Structures*, **63**: 39-50.

Brenner, D. W. (1990): Empirical potential for hydrocarbons for use in simulating the chemical vapor decomposition of diamond films. *Physical Review B* **42**: 15.

Brenner, D. W.; Shenderova, O. A.; Areshkin, D. A.; Schall, J. D.; Frankland, S.J.V. (2002): Atomic modeling of carbon-based nanostructures as a tool for developing new materials and technologies. *CMES: Computer Modeling in Engineering & Science* **3** (5): 643-673.

Chen, W.H.; Cheng, H.C.; Hsu, Y.C. (2007): Mechanical Properties of Carbon Nanotubes Using Molecular Dynamics Simulations with the Inlayer van der Waals Interactions. *CMES: Computer Modeling in Engineering & Sciences* **20** (2): 123-145.

Civelek, M.B., Erdogan, F., Cakiroglu, A.O. (1978): Interface separation for an elastic layer loaded by a rigid stamp. *Int. J. Engng. Sci*. **16** (9): 669–679.

Chiroiu, V.; Munteanu. L.; Donescu, St. (2006): On the mechanical modeling of single-walled carbon nanotubes. *Rev. Roum. Sci,. Techn., Serie Mécanique Appl*. **51** (1): 37-52.

Chollacoop, B. (2004): *Computational and Experimental Study of Instrumented Indentation*. Phd Thesis: Massachusetts Institute of Technology.

Dumitriu, D.; Chiroiu, V. (2006): On the Dual Equations in Contact Elasticity. *Rev. Roum. Sci,. Techn., Serie Mécanique Appl*. **51** (3): 261-272.

Dumitriu, D.; Chiroiu, V. (2008): On the Modeling of Nanocontacts, *Rev. Roum. Sci. Techn., Serie Mécanique Appl*. **53** (3).

Dumitriu, D.; Gauchs, G.; Chiroiu, V. (2008): Optimisation Procedure for Parameter Identification in Inelastic Material Indentation Testing, *Rev. Roum. Sci. Techn., Serie MéCanique Appl*. **53** (1): 43-54.

Eringen, A.C. (1974): *On nonlocal continuum thermo-dynamics. Modern developments in thermodynamics*, (ed. B. Gal-Or), New York: John Wiley and Sons, 121-142.

Eringen A.C. (1977): Continuum mechanics at the atomic scale, *Crystal Lattice Defects*, **7**, 109–130.

Eringen, A.C. (2002): *Nonlocal Continuum Field Theories*, Springer.

Guz, A.N.; Rushchitsky, J.J.; Guz, I.A. (2008): Comparative Computer Modeling of Carbon-Polymer Composites with Carbon or Graphite Microfibers or Carbon Nanotubes. *CMES: Computer Modeling in Engineering & Science* **26** (3): 139-156.

Hu, S.; Shen, S. (2008): Analysis of the interaction between two nanovoids using bipolar coordinates. *CMES: Computer Modeling in Engineering & Science* **30** (2): 57-64.

Jiang, H.; Lu, J.; Yu, M.-F. (2008): Carbon Nanotube Transmission between Linear and Rotational Motions. *CMES: Computer Modeling in Engineering & Science* **24** (2) 95-102.

Johnson, K.L. (1985*): Contact Mechanics,* Cambridge University Press, New York.

Kiang,C.H.; Endo, M.; Ajayan, P.M.; Dresselhaus, G.; Dresselhaus, M.S. (1998): Size effects in Carbon Nanotubes. *Physical Review Letters* **81** (2): 1869-1872.

Li, C. Y.; Chou, T.W. (2003): Elastic moduli of multi-walled carbon nanotubes and the effect of van der Waals forces. *Composite Science and Technology*, **63**: 1517-1524.

Ling, X.; Atluri, S.N. (2007): A Hyperelastic Description of SingleWall Carbon Nanotubes at Moderate Strains and Temperatures. *CMES: Computer Modeling in Engineering & Sciences* **21** (1): 81-91.

Liu, C.-S. (2008): Improving the Ill-conditioning of the Method of Fundamental Solutions for 2D Laplace Equation. *CMES: Computer Modeling in Engineering & Sciences* **28** (2) 77-93.

Nair, A.K.; Farkas, D.; Kriz, R.D. (2008): Molecular Dynamics Study of Size Effects and Deformation due to Nanoindentation. *CMES: Computer Modeling in Engineering & Sciences* **24** (3): 239-248.

Qian, D.; Wagner, G. J.; Liu, W. K.; Yu, M. F.; Ruoff, R. S. (2002): Mechanics of carbon nanotubes. *Appl. Mech. Rev.* **55** (6).

Oliver, W.C.; Pharr, G.M. (1992): Improved technique for determining hardness and elastic modulus using load and displacement sensing indentation experiments. *Journal of Materials Research* **7** (6): 1564–1580.

Solano C.J.F.; Costales A.; Francisco E.; Pendáas A.M.; Blanco M.A.; Lau K.C.; He H., Pandey R. (2008): Buckling in Wurtzite-Like AIN Nanostructures and Crystals: Why Nano can be Different. *CMES: Computer Modeling in Engineering & Sciences* **24** (2): 143-156.

Solomon, L. (1964): Upon the geometrical punch-penetration rigidity. *Lincei-Rend. Sc. Fis. Mat. E Nat*. **36**: 832–835.

Srivastava, D.; Atluri, S.N. (2002): Computational Nano-technology: A Current Perspective. *CMES: Computer Modeling in Engineering & Sciences* **3** (5): 531-538.

Theodosiou, T.C.; Saravanos, D.A. (2007): Molecular Mechanics Based Finite Element For Carbon Nanotube Modeling. *CMES: Computer Modeling in Engineering & Sciences* **19** (2): 121-134.

Wang, H.T.; Yao, Z.H. (2008): A Rigid-fiber-based Boundary Element Model for Strength Simulation of Carbon Nanotube Reinforced Composites. *CMES: Computer Modeling in Engineering & Sciences* **29** (1): 1-13.

Waters, J.F.; Guduru, P.R.; Jouzi, M.; Xu, J.M. (2005): Shell buckling of individual multiwalles carbon nanotubes using nanoindentation. *Applied Physics Letters* **87**: 103109.

Yang, B.; Wong, S.-C.; Qu, S. (2008): A Micromechanics Analysis of Nanoscale Graphite Platelet-Reinforced Epoxy Using Defect Green's Function. *CMES: Computer Modeling in Engineering & Sciences* **24** (2): 81-93.